The predicted effect of preservation scenarios on indoor overheating for the renovation of heritage-listed apartment-style lilong houses in Shanghai under climate change

Lei, Muxi; van Hooff, Twan; Blocken, Bert; Pereira Roders, Ana

DOI
10.1186/s43238-025-00183-2

Publication date
2025

Document Version
Final published version

Published in
Built Heritage

Lei *et al. Built Heritage* (2025) 9:16
https://doi.org/10.1186/s43238-025-00183-2

Built Heritage

RESEARCH ARTICLE

Open Access

The predicted effect of preservation scenarios on indoor overheating for the renovation of heritage-listed apartment-style *lilong* houses in Shanghai under climate change

Muxi Lei[1,2*], Twan van Hooff[1], Bert Blocken[3,4] and Ana Pereira Roders[5]

Abstract

An increase in ambient air temperature due to climate change can adversely affect indoor thermal conditions, particularly in heritage-listed dwellings, as renovation efforts may be limited by preservation constraints, potentially leading to indoor overheating for occupants. Incorporating heritage-listed dwellings into the climate change adaptation strategies is essential. Heritage-listed dwellings exhibit varying preservation constraints, with character-defining elements differing across cases. A literature review indicates a deficiency in research regarding climate change adaptation for *lilong* houses, which are two- to three-storey terrace houses featuring timber-brick structures, predominantly constructed in late 19th and early 20th century Shanghai, and recognised as significant urban heritage of the city. Through building energy simulations, this article examines the climate change adaptation of heritage-listed apartment-style *lilong* houses in Shanghai. Overheating hours and degree hours are utilised to assess indoor overheating conditions. Three scenarios for the preservation of the building envelope are proposed: (1) preservation of walls, (2) preservation of windows, (3) preservation of the roof. There are five categories of climate change adaptation measures. The findings indicate that substantial reductions can be attained by implementing a single preservation scenario customised to the character-defining elements and preservation constraints of heritage-listed dwellings. The most significant decrease in the number of overheating hours is observed in the wall preservation scenario, with a reduction of 69%, followed by a 53% reduction in the roof preservation scenario and a 31% reduction in the window preservation scenario. The proposed preservation scenarios enable the improvement in building indoor thermal conditions without compromising heritage preservation.

Keywords Shanghai, Heritage-listed dwellings, Apartment-style *lilong* houses, Indoor overheating, Future climate, Climate change adaptation, Building renovation

*Correspondence:
Muxi Lei
m.lei@tue.nl
Full list of author information is available at the end of the article

1 Introduction

In line with global trends, due to climate change, the near-surface air temperature in China increased by 0.24 °C /10 years from 1951 to 2018 (Climate Change Center of CMA, 2019), with future increases predicted within a range of 1.3 °C to 5.0 °C for the period 2081 to 2100 compared to the period 1986 to 2005 (CTNARCC Editorial Committee, 2015). The predicted increase in ambient air temperature can lead to increased indoor overheating, resulting in thermal discomfort for the occupants.

Building renovations can improve the performance of buildings in indoor thermal conditions (e.g. van Hooff et al. 2014; Vasaturo et al. 2018). However, heritage-listed dwellings often have preservation constraints (e.g. Martínez-Molina et al. 2016), which may disable the needed improvements in the renovations. Thus, climate change may have a long-term impact on the health and well-being of occupants. Preservation concerns the process of 'maintaining a place in its existing state and retarding deterioration' (Australia ICOMOS, 2013, 2). These preservation constraints are important as they preserve the character-defining elements conveying cultural significance over time. Thus, adapting heritage-listed dwellings to future climate change is important yet challenging, particularly regarding the maintenance of both occupant thermal comfort and character-defining elements. Considering heritage-listed dwellings differ in preservation constraints, where the character-defining elements vary per building, it is important to research the potential of improving building performance at the level of the building components (e.g. De Berardinis et al. 2014). Because, for example, in heritage-listed dwellings where the roof conveys significance, other building components as the walls and windows could be improved.

Earlier studies have investigated the predicted effect of future climate change on indoor thermal conditions. A study for dwellings in Lisbon, Portugal, showed a predicted increase in discomfort hours of 13% to 17% for 2050 and 43% to 53% for 2080 compared to a typical meteorological year (TMY) (Barbosa et al. 2015). Yu et al. (2023) showed an increase in overheating hours from 884 h for a TMY to 1719 h for 2060 for a residence in Changchun, China, due to the predicted climate change. Conversely, indoor thermal conditions can be improved (e.g. Jafarpur and Berardi 2021), mainly depending on the local climate conditions and the season studied. Applying climate change adaptation measures (CCAMs) can provide a solution to reduce indoor overheating in buildings under climate change (e.g. van Hooff et al. 2014; Albers et al. 2015; Baba et al. 2023).

The usability of heritage-listed dwellings may be compromised due to a decrease in indoor thermal comfort resulting from climate change (e.g. Muñoz González et al. 2020; Lei et al. 2022). Regarding indoor thermal conditions, Muñoz González et al. (2020) showed that a decrease in discomfort hours of 10% to 20% during cold months and an increase of 20% to 30% during warmer months were predicted in 2050 compared to 2018 for historic churches in Seville, Spain. Moreover, Lei et al. (2022) predicted an increase of 58% to 60% in the number of overheating hours for Beijing and 41% to 44% for Shanghai for a heritage-listed dwelling in 2050 compared to a TMY. These previous studies showed that climate change could have noticeable effects on heritage-listed dwellings and thus may compromise the cultural significance of buildings. In addition, poor indoor thermal conditions can be present, leading to possible unwanted/uncontrolled building renovation, changes in room usage, or even abandoned heritage-listed dwellings. It is necessary to mitigate the adverse effects of climate change, for example, on indoor thermal conditions in heritage-listed dwellings. However, none of the aforementioned studies focused on climate change adaptation of traditional *lilong* houses, which are two- to three-storey terrace houses featuring timber-brick structures, predominantly constructed in late 19th and early 20th century Shanghai, and recognised as significant urban heritage of the city. This is notable given the increasing interest in enhancing thermal comfort in *lilong* houses (e.g. Song and Mo 2010).

2 Base case building: generic heritage-listed dwellings

This article takes apartment-style *lilong* houses as an example to evaluate indoor overheating and its mitigation under climate change using building energy simulations. Apartment-style *lilong* houses in Shanghai were built around the 1940s (Xu and Yan 1983), prior to the introduction of the first Chinese building energy standard in the 1980s (Chen et al. 2015). This building type typically consists of a two- to three-storey timber-brick structure. It is characterised by a compact interior, often lacking a parlor room (Xue and Lou 2005), and low thermal resistance in the building envelope due to insufficient thermal insulation (Song and Chen 2010). Yongjia New Village (Yongjia Xincun) was defined as a generic building model which served as the base case (i.e. without CCAMs implemented) (e.g. Xu and Yan 1983). It was built with a site area of around 3.7 hm^2 in the 1940s (Lou and Xue 2002) and was listed as the second batch of 'Outstanding Historic Building' in 1994 (Office of Shanghai Chronicles 2005).

The typical layout of the dwelling is shown in Fig. 1. The number of floors, building geometry, interior layout and bedroom dimensions of the generic model were

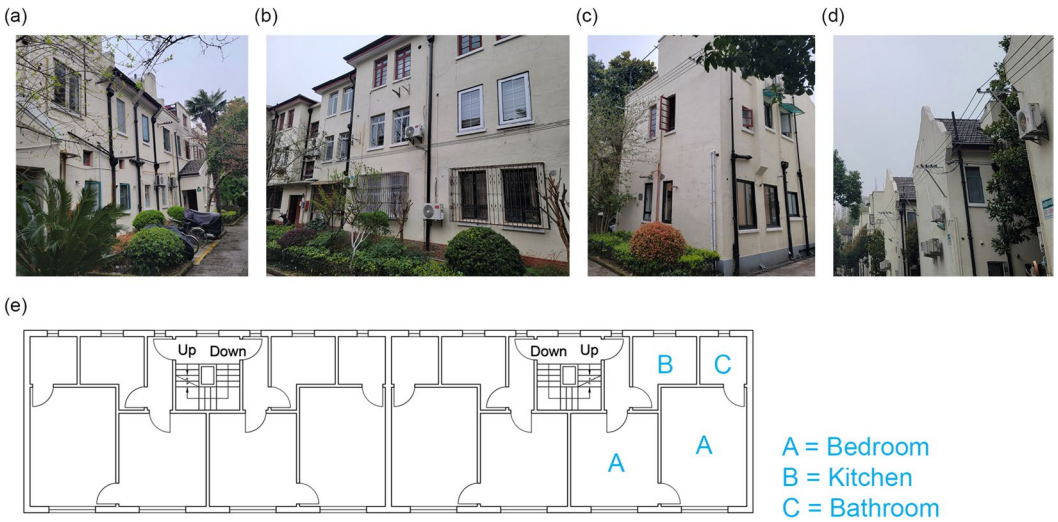

Fig. 1 Shanghai Yongjia New Village (Yongjia Xincun). **a**, **b** Building facades, **c** windows, **d** roof attic, **e** indication of the interior layout for a dwelling on the 1st floor [Source: the authors. Subfigure (**e**) is based on Xue and Lou (2005), Lianjia (2016) and on-site investigation]

based on data identified from (Xue and Lou 2005) and from the online real estate platform Lianjia (Lianjia 2016) (Fig. 2). The building has a timber-brick structure with construction and materials summarised in Table 1. An assumption was made about the dimension of the air cavity for modelling (see Table 1). The occupancy schedule of a working couple was based on the work of Hu et al. (2019). Details of the occupancy schedule and internal heat gains are shown in Table 2.

3 Building envelope preservation and climate change adaptation measures

3.1 Scenarios for building envelope preservation

Indoor building thermal conditions are largely affected by building envelope properties, while constraints on the renovation of certain character-defining elements may be present due to preservation constraints for heritage-listed dwellings. For Yongjia New Village, the character-defining elements include the building envelope and the

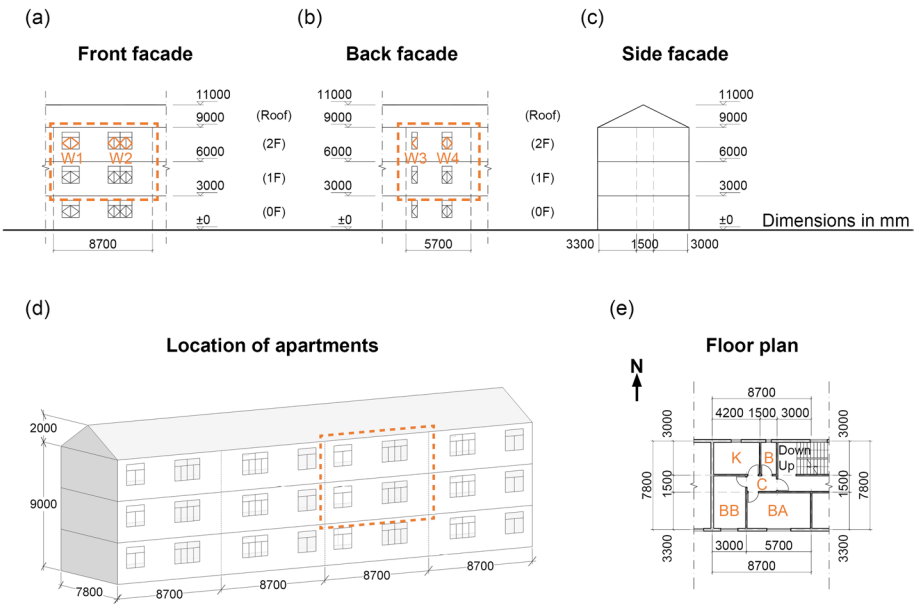

Fig. 2 Generic building based on Xue and Lou (2005) and Lianjia (2016). **a**-**c** Front facade, back facade and side facade. W1 to W4 show the operable windows (same for all floors). The dashed box in (**a**, **b**, **d**) shows the location of the studied dwellings. The ground floor was not included to avoid ground effects on the heat balance. **e** Floor plan and interior layout: Bedroom A (BA), Bedroom B (BB), Corridor (C), Kitchen (K) and Bathroom (B). Dimensions in millimetres (Source: the authors)

Table 1 Building construction and materials based on Lou and Xue (2002), Xue and Lou (2005) and Song and Chen (2010)). Values for the thermal resistance of the construction (R_c) were based on CIBSE (2015) and MOHURD and AQSIQ (2016)

Building components	Construction (from outside to inside)[a]	Thermal resistance of construction (R_c) [m^2K/W]
Internal floor/ceiling	Timber deck, air cavity (d (cavity width) = 150 mm, R_{cav} (thermal resistance of the cavity) = 0.19 m^2K/W (CEN, 2007)), timber deck	0.43
Ground floor	Rammed earth, concrete, cement mortar (floor/ceiling)	1.14[b]
Pitched roof	Clay tiles, timber roof deck	0.17
Doors	Timber doors	0.23
Windows[c]	Single-pane glazing with wooden frames (thermal transmittance value (U value) = 5.20 W/m^2K, solar heat gain coefficient = 0.70 (ASHRAE, 2021))	-
External walls	Plaster, bricks (external), cement mortar (wall)	0.39
Internal walls	Cement mortar (wall), bricks (internal), cement mortar (wall)	0.21

[a] 0.3 was set for solar reflectivity value (albedo) except for the plaster (albedo = 0.9 for the plaster), and 0.9 was set for thermal emissivity value for all the opaque materials (e.g. Bretz et al. 1992)

[b] Monthly ground temperatures at 1.0 m depth were used (Meteotest 2021)

[c] A fixed window was used if the window conveys cultural significance

Table 2 Room occupied hours and internal heat gains

Rooms	Heat gains[a]	Monday to Friday	Weekends
Bedroom A	Occupant, electric equipment, lighting	7:00–7:30 h, 18:00–22:30 h	9:00–9:30 h, 12:00–13:00 h, 19:00–23:00 h
Bedroom B	Occupant, electric equipment	0:00–6:30 h, 22:30–24:00 h	0:00–8:30 h, 13:00–15:00 h, 23:00–24:00 h
Kitchen	Occupant, electric equipment, lighting, gas equipment, refrigerator	6:30–7:00 h, 17:00–18:00 h	8:30–9:00 h, 11:00–12:00 h, 18:00–19:00 h

[a] Heat gains from occupant for Bedroom A = 126 W (male) & 112 W (female), Bedroom B = 72 W (male) & 64 W (female), Kitchen = 167 W (male) & 149 W (female) (AQSIQ and SAC 2008; MOHURD and AQSIQ 2012a). Electric equipment = 3.8 W/m^2 and lighting = 5 W/m^2 (MOHURD 2018). Gas equipment = 1000 W and a refrigerator = 60 W (e.g. Hasan et al. 2009; ASHRAE 2021). Note that 10% of the electric equipment load was present for Bedroom B (e.g. Lam et al. 2005), lighting only after 17:00 h and the heat gain from the refrigerator for the entire day

featured interior decoration (Xuhui District Housing Security and Administration Bureau 2016). Hence, building envelope preservation is considered in the present study to minimise the effect on envelope components conveying cultural significance.

Measures to improve the indoor thermal conditions and reduce energy demand may still be applicable, e.g. on a building component level such as walls, windows, roofs, etc., depending on the character-defining elements and the limits of acceptable change (e.g. De Berardinis et al. 2014; Standing Committee of SMPC, 2019). An earlier study showed that the preservation constraints of the envelope components of *lilong* houses vary; modifications are restricted for certain external walls, while alterations are permitted for those that have previously undergone changes (e.g. Song and Mo 2010).

A scenario-based approach was adopted to address the diverse preservation constraints. Three essential components of the building envelope, i.e. walls, windows and roof, were considered based on which three preservation scenarios were developed. In order to minimise the potential impact of CCAMs on the original architectural appearance, no CCAMs were applied to the component to be preserved:

- Wall preservation scenario: external walls are preserved, while windows and the roof are adapted for better performance in the building renovation.
- Window preservation scenario: windows are preserved, while external walls and the roof are adapted for better performance in the building renovation.
- Roof preservation scenario: the roof is preserved, while external walls and windows are adapted for better performance during the building renovation.

3.2 The considered climate change adaptation measures

Five types of CCAMs were included in the present study: (1) lower thermal transmittance, (2) vegetated roof, (3) increased roof solar reflectance, (4) adding exterior solar shading, and (5) additional natural ventilation.

In CCAM 1, for lower thermal transmittance, increased wall insulation (RC_wall), increased roof insulation

(RC_roof) and window replacement (WR) were studied. For energy saving, an insulation layer of extruded polystyrene with a thickness of 120 mm was added for RC_wall and RC_roof. The insulation layer for RC_wall was added at the outer surface of the external walls, i.e. external insulation, to minimize possible condensation due to thermal bridges (MOHURD, 2012). External insulation, however, is not suggested to be applied to the external walls with cultural significance. For RC_roof, the insulation layer was added between the clay tile and the roof deck. For WR, a window with a visible transmittance value of 0.50 (ASHRAE 2021), which is larger than 0.45 as required by MOHURD and AQSIQ (2012b), was used, which has a solar heat gain coefficient of 0.34 (see Table 3). WR was only included for the case where the original windows were replaced to minimize its effect on the cultural significance of the heritage-listed dwellings. The thermal transmittance values (U values) of the different envelope parts with CCAMs implemented were smaller than the U values required by the relevant guidelines (MOHURD, 2010, 2012) (see Table 3).

In CCAM 2, an extensive vegetated roof (VR) was used, consisting of a reinforced concrete deck with 0.25 m thickness of substrate and soil, supporting a ground cover plant (sedum) (MOHURD 2013). The VR construction, including vegetation, substrate, roofing material and roof deck, was based on MOHURD (2013) and CIBSDR (2014) (see Table 3). The application of VR may require additional renovation actions, which could change the original architectural appearance, especially for the roof conveying cultural significance.

In CCAM 3, for increased roof short-wave reflectance (SR09_roof), the short-wave reflectivity or albedo value of the outer surface of the roof was increased to 0.9 using high-solar reflecting coatings.

In CCAM 4, a movable vertical roller shade providing exterior solar shading (SS) was used at the windows (see Table 3). If activated, all of the glazing areas of a window will be covered by the shading (U.S. Department of Energy, 2019c).

In CCAM 5, additional natural ventilation (NV) can be readily implemented through windows (NV_window) for wall and roof preservation scenarios, with ventilation flow rate dependent on wind speed and thermal stack effect (U.S. Department of Energy, 2019c). For the window preservation scenario, however, no natural ventilation was provided through the windows, i.e. a 'worst case' scenario with the windows closed, and thus building openings on the external walls, e.g. wall grilles (NV_wall) and opened doors were used instead to provide natural

Table 3 Overview of the considered climate change adaptation measures (CCAMs)

Building renovation	Climate change adaptation measures
Increased wall insulation (RC_wall)	U = 0.25 W/m^{2}K (i.e. < 1.5 W/m^{2}K as required by (MOHURD, 2010, 2012))[a]
Increased roof insulation (RC_roof)	U = 0.27 W/m^{2}K (i.e. < 0.8 W/m^{2}K as required by (MOHURD, 2010, 2012))[a]
Window replacement (WR)	U = 1.52 W/m^{2}K (i.e. < 4.0 W/m^{2}K as required by (MOHURD, 2010, 2012)), solar heat gain coefficient = 0.34 (ASHRAE, 2021)
Vegetated roof (VR)[b]	• Vegetation: height = 0.10 m (Peng and Yang 2019), leaf area index (LAI) = 4 (Sailor and Bass 2014), leaf albedo value = 0.17 (Feng et al. 2010) • Substrate: thickness = 0.25 m (MOHURD 2013), R = 1.25 m^{2}K/W for dry soil • Roofing materials: thickness = 0.07 m, R = 0.17 m^{2}K/W • Roof deck: thickness = 0.20 m, R = 0.11 m^{2}K/W
Increased roof short-wave reflectance (SR09_roof)	Short-wave reflectivity (albedo) value was increased from 0.3 to 0.9 for the outer surface of the roof (e.g. Bretz et al. 1992)
Exterior solar shading Vertical roller shade (SS)	Solar reflectivity value = 0.8 (e.g. Bretz et al. 1992), distance between shading and glazing = 0.05 m (U.S. Department of Energy, 2019c) Two activation criteria: • Incident solar irradiance on windows > 200 W/m^2 (e.g. Beck et al. 2010; U.S. Department of Energy 2019a, 2019b) • Indoor air temperature > 20 °C (i.e. 2 °C higher than the heating setpoint from (MOHURD, 2010))
Additional natural ventilation through windows (NV_window) or wall openings (NV5_wall)	Two ventilation conditions: • Available for daytime only (7:00–19:00 h for weekdays and 9:00–20:00 h for weekends), i.e. NV_window_day & NV5_wall_day • Available for a whole day, i.e. NV_window_day + night & NV5_wall_day + night Two criteria: • Indoor air temperature > 26 °C (i.e. same as the cooling setpoint from (MOHURD, 2010)) • Outdoor air temperature < indoor air temperature (e.g. van Hooff et al. 2014)

[a] R_e (exterior surface heat transfer resistance) = 0.05 m^2 K/W, R_i (interior surface heat transfer resistance) = 0.11 m^2 K/W (MOHURD and AQSIQ 2016) for the estimation of U (thermal transmittance) values, in EnergyPlus these values are not used but external and internal convective heat transfer coefficients were calculated using DOE-2 and TARP, respectively (Walton 1983; LBL 1994; Mirsadeghi et al. 2013; U.S. Department of Energy 2019b, 2019c)

[b] R (thermal resistance) values were based on Tang et al. (2007), CIBSE (2015) and MOHURD and AQSIQ (2016)

cross-ventilation with an average ventilation flow rate of 5.0 h^{-1} air changes per hour (ACH) (based on an average wind speed of 3.7 m/s (Meteotest 2021) and an opening area of 0.1 m^2). Table 3 shows the conditions and criteria for introducing natural ventilation.

In addition, the individual CCAMs in different preservation scenarios were combined to evaluate their effectiveness. Table 4 shows the selection and combination of the CCAMs in different preservation scenarios. The combined CCAMs, if used at the same location, were determined based on the most effective individual measure for that location, e.g. SR09_roof instead of VR for the roof. Note that the combined measures are based on the selected individual CCAMs in different preservation scenarios, as shown in Table 4, to achieve a possible largest reduction in indoor overheating. Multiple preservation scenarios merged or combined with all individual CCAMs would require additional analyses.

4 Methodology

4.1 Weather conditions

Weather data of a TMY (air temperature of 2000–2019; solar radiation of 1991–2010) generated from Meteonorm (Meteotest 2021) was used to represent the current climate. The future weather data in 2050 was stochastically generated using Meteonorm (Meteotest 2020b, 2021) to represent the near-term future climate (hereinafter 2050). The future climate data was generated under the climate change scenario of representative concentration pathway (RCP) with the highest emission level, i.e. RCP8.5 (Moss et al. 2010; van Vuuren et al. 2011), based on an average of 10 Coupled Model Intercomparison Project Phase 5 global climate models (Meteotest 2020a).

Figure 3a shows a clear increase in the predicted annual and monthly average ambient air temperatures in Shanghai. The annual average air temperature in 2050 ($T_{avg,2050}$) is predicted to be 2 °C higher than in the TMY ($T_{avg,TMY}$). Furthermore, the monthly average air temperature in each month is higher in 2050 than in the TMY, with the increase ranging from 1.5 °C to 2.4 °C. The percentual change in the annual average hourly solar radiation is small, i.e. $\Delta G_{h,a} = +7.3\%$ (Fig. 3a). Figure 3b shows an increase in the number of hours with an air temperature higher than 30 °C ($\Delta n_{30} = 420$) and 35 °C ($\Delta n_{35} = 256$) for 2050 compared to the TMY during the summer (1 June to 31 August).

4.2 Simulation settings

Building indoor thermal conditions were simulated using EnergyPlus (Crawley et al. 2001; U.S. Department of Energy 2019a). The number of time steps per hour was set to 6, except for VR. For VR, the number of time steps per hour was increased to 60, as suggested by the U.S. Department of Energy (2019c). A ventilation rate of 1.0 h^{-1} was provided to the bedrooms for the entire day (MOHURD, 2010), and a ventilation rate of 11.9 h^{-1} (450 m^3/h) for the kitchen during the occupied hours (e.g. CECS 2010). The infiltration rate of 0.645 h^{-1} used for all the rooms, including the roof attic, was averaged from Chen et al. (2012) and Shi et al. (2015). Ground reflectivity values were set to 0.2 throughout the year (e.g. Liu and Jordan 1963; Thevenard and Haddad 2006). Heating was provided during the heating period from 1 December to 28 February (MOHURD 2010). Indoor overheating was only evaluated during the non-heating period, i.e., 1 March to 30 November (6600 h). Adiabatic walls were assumed for the walls between the studied dwelling and the neighbouring dwellings, while the floor and ceiling were influenced by the indoor conditions of the dwellings located above and below the target dwelling. The suitability of the simulation settings was validated in the study of Lei et al. (2022) based on a comparison with experimental data from the literature. Bedroom windows were

Table 4 Implementation of the CCAMs on the developed envelope preservation scenarios

	Preservation scenarios		
	Wall preservation	**Window preservation**	**Roof preservation**
Envelope component			
CCAMs for wall[a]	(-)	RC_wall, NV5_wall_day, NV5_wall_day + night	RC_wall
CCAMs for window[a]	NV_window_day, NV_window_day + night, WR, SS	(-)	NV_window_day, NV_window_day + night, WR, SS
CCAMs for roof[a]	RC_roof, VR, SR09_roof	RC_roof, VR, SR09_roof	(-)
Combined measures	NV_window_day + night, WR, SS, RC_roof, SR09_roof	NV5_wall_day + night, RC_roof, SR09_roof	NV_window_day + night, WR, SS

[a] (-): no measures implemented. RC_wall: increased wall insulation. RC_roof: increased roof insulation. WR: window replacement. VR: vegetated roof. SR09_roof: increased roof short-wave reflectance. SS: exterior solar shading. NV_window_day/day + night: additional natural ventilation through windows. NV5_wall_day/day + night: additional natural ventilation through wall openings

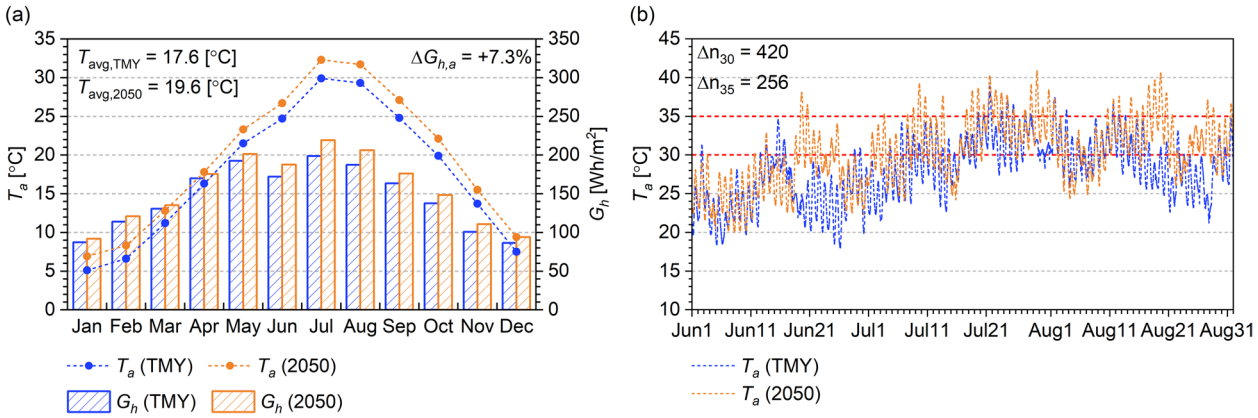

Fig. 3 Air temperature (T_a) and hourly solar radiation (G_h) in the typical meteorological year (TMY) and 2050 in Shanghai. In (**a**), the dots represent the monthly average air temperatures, and the bars represent the monthly average hourly solar radiation. Hourly air temperatures from 1 June until 31 August are shown in (**b**). The horizontal dashed lines in (**b**) indicate the air temperature of 30 °C and 35 °C. Note that the axis in (**b**) starts from a non-zero value of 10 °C (Source: the authors)

orientated towards eight different orientations, i.e., the south (S), southwest (SW), west (W), northwest (NW), north (N), northeast (NE), east (E) and southeast (SE), to include the effect of orientation on indoor overheating.

4.3 Assessment of indoor overheating

A Chinese adaptive thermal comfort model from the guideline GB/T 50785–2012 (MOHURD and AQSIQ 2012a) was selected to evaluate occupant thermal comfort. The adaptive thermal comfort model was selected for a Chinese hot summer and cold winter climate zone (e.g. Shanghai (MOHURD and AQSIQ 2016)).

The running mean outdoor temperature was calculated using Eq. (1) (MOHURD and AQSIQ 2012a):

$$T_{rm} = (1-\alpha)\left(T_{od-1} + \alpha T_{od-2} + \alpha^2 T_{od-3} + \alpha^3 T_{od-4} + \alpha^4 T_{od-5} + \alpha^5 T_{od-6} + \alpha^6 T_{od-7}\right) \quad (1)$$

with.

T_{rm} = running mean outdoor temperature [°C];

α = 0.8;

$T_{od\text{-n}}$ = daily average outdoor temperature of n days ago [°C].

4.3.1 Indoor overheating hours

The upper threshold of category II (75% to 90% acceptability (Carlucci et al. 2018) from the guideline GB/T 50785–2012 was selected to evaluate indoor overheating conditions using Eq. (2) (MOHURD and AQSIQ 2012a):

$$T_{upper} = 0.73 T_{rm} + 12.72 \quad (2)$$

with.

T_{upper} = upper threshold of the indoor operative temperature [°C] (18 °C ≤ T_{upper} ≤ 30 °C);

T_{rm} = running mean outdoor temperature [°C].

The hourly overheating condition was determined by Eq. (3).

$$oh_i = \begin{cases} 1, & T_o > T_{upper} \\ 0, & T_o \le T_{upper} \end{cases} \quad (3)$$

with oh_i the hourly overheating conditions, T_o is the indoor operative temperature [°C] (ASHRAE, 2021), T_{upper} the upper threshold of the indoor operative temperature [°C].

The number of overheating hours was calculated using Eqs. (3) and (4):

$$h_o = \sum_{i=1}^{n} (oh_i \Delta t) \quad (4)$$

with h_o the overheating hours [h], n is the number of hours during the non-heating period, i.e. 6600, oh_i the hourly overheating condition, Δt one hour [h].

4.3.2 Indoor degree hours for the evaluation of overheating

The degree of overheating was indicated by the number of degree hours using Eq. (3) and Eq. (5).

$$h_d = \sum_{i=1}^{n} [oh_i (T_o - T_{upper}) \Delta t] \quad (5)$$

with h_d the degree hours [°Ch], n the number of hours during the non-heating period, i.e. 6600, oh_i the hourly overheating conditions, T_o is the indoor operative temperature [°C], T_{upper} the upper threshold of the indoor operative temperature [°C] and Δt one hour [h].

5 Results

5.1 Base case dwellings

Figure 4 shows the predicted number of overheating hours (Fig. 4a, b) and degree hours (Fig. 4c, d) for the bedrooms of the base case dwellings under future climate change. The number of overheating hours and degree hours is larger for all orientations in 2050 compared to the TMY due to the predicted increase in the ambient air temperature in 2050. Furthermore, the average number of overheating hours and degree hours increases for 2050 compared to the TMY, ranging from 28 to 32% for the average number of overheating hours and from 69 to 84% for the average number of degree hours.

The largest number of overheating hours and degree hours occurs when the bedroom windows are oriented towards the eastern sides (SE or E for the number of overheating hours; E for the number of degree hours).

The number of overheating hours and degree hours for each orientation is, as expected, smaller for the bedrooms on the 1st floor compared to the 2nd floor. This is because of the low albedo value (albedo = 0.3 (see Sect. 2)) and the limited thermal resistance of the roof surface, i.e. larger transmission heat gains for the attic and the limited thermal resistance of the ceiling between the attic and the dwelling on the 2nd floor, resulting in an increased heat gain by the transmission for the dwelling on the 2nd floor. Therefore, the dwelling on the 2nd floor has a higher indoor overheating risk than the 1st floor. This observation is in line with the specific suggestion for an evaluation of summer indoor thermal conditions after renovation for the rooms on the top floor in the Chinese hot summer and cold winter climate zone by MOHURD (2012). Therefore, the remainder of this study focuses on the effect of CCAMs on indoor overheating in the dwelling on the 2nd floor.

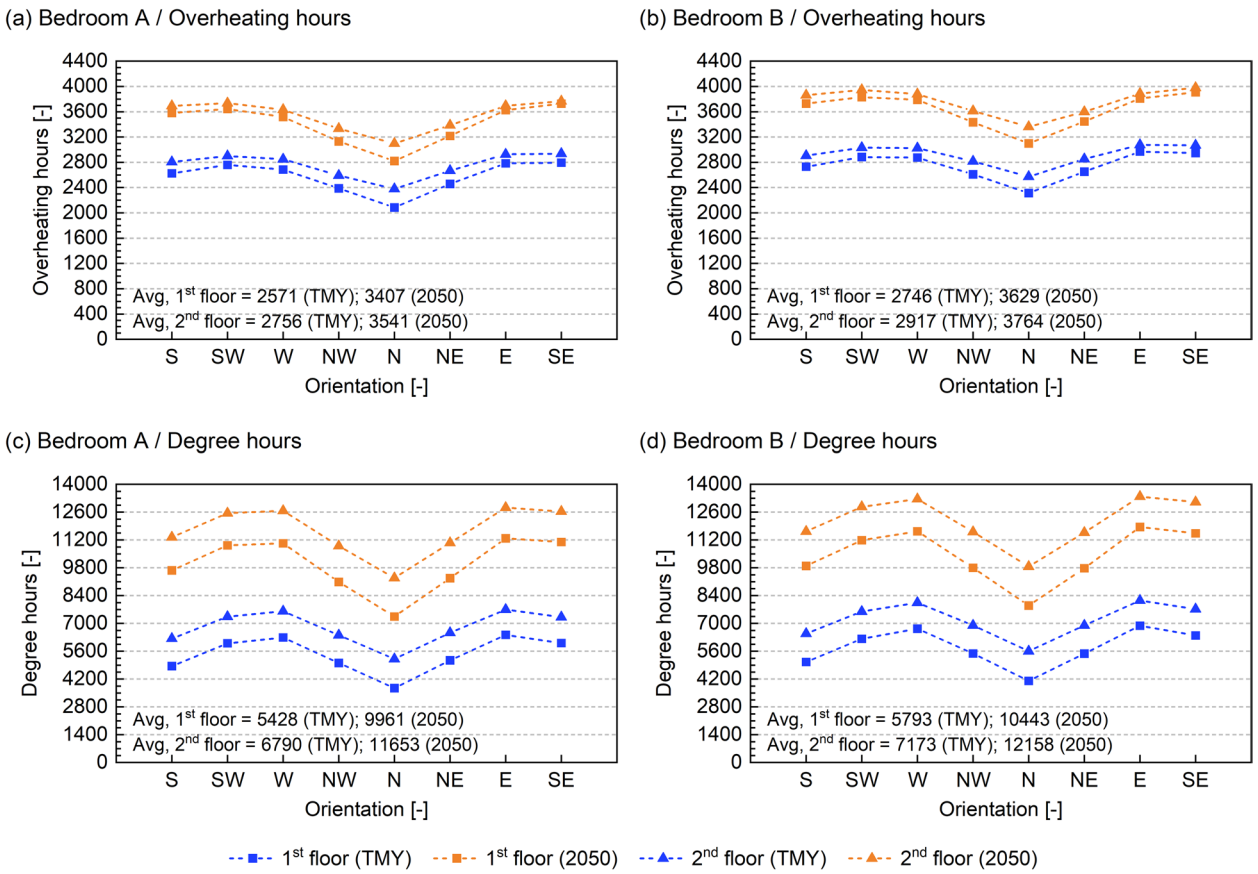

Fig. 4 The number of overheating hours for (**a**) Bedroom A and (**b**) Bedroom B, and the number of degree hours for (**c**) Bedroom A and (**d**) Bedroom B in the TMY and 2050. The average numbers over the eight orientations for the 1st floor (Avg, 1st floor) and the 2nd floor (Avg, 2nd floor) are indicated at the bottom of each graph (Source: the authors)

5.2 Effect of climate change adaptation measures

Numerical simulations for the effects of the CCAMs were performed for both Bedroom A and Bedroom B, and the simulation results are similar between Bedroom A and Bedroom B. Hence, the results are only reported for brevity in Bedroom A.

5.2.1 Wall preservation scenario

Figure 5 compares the average, maximum and minimum numbers of overheating hours (Fig. 5a) and degree hours (Fig. 5b) before and after the implementation of the CCAMs in the wall preservation scenario. In Fig. 5, the columns show the average values, and the error bars represent the maximum and minimum values of the eight orientations.

CCAMs for window: Additional natural ventilation through the windows available for a whole day (NV_window_day + night) achieves a larger reduction in the number of overheating hours and degree hours compared to daytime only (NV_window_day). WR and using exterior SS show similar reductions in the average number of overheating hours and degree hours. However, the application of SS results in the smallest difference between the maximum and minimum numbers of overheating hours and degree hours. Thus, the effect of this CCAM on overheating is less dependent on orientation.

CCAMs for roof: RC_roof only leads to a marginal decrease in the average number of overheating hours and degree hours due to the reduced heat loss through the roof attic during the night, which partly counteracts the effect of RC_roof to reduce transmission heat gains during daytime. In addition, almost no effect (≤ 2%) on the average number of overheating hours and only a small reduction in the average number of degree hours are found when applying VR. The small decrease can be explained by the lower albedo of the leaf (0.17 for the leaf and 0.3 for the roof surface (see Sect. 2 & 3)), the dwelling location (the dwelling is not directly under VR) and the considered vegetation type (an extensive vegetated roof was used instead of an intensive one), which together limit the effect of VR. SR09_roof effectively reduces the average number of overheating hours (−26% for TMY; −21% for 2050) and degree hours (−41% for TMY; −33% for 2050).

Combined window and roof CCAMs: The implementation of the combined window and roof CCAMs results in a considerable reduction in the average number of overheating hours (−69% for TMY; −62% for 2050) and degree hours (−85% for TMY; −76% for 2050).

In the wall preservation scenario, the most effective individual climate change adaptation measure to reduce the average number of overheating hours and degree hours is NV_window_day + night. The combined window and roof CCAMs are more effective than the individual CCAMs in terms of reducing the average number of overheating hours and degree hours and can limit the number of hours to 867 (TMY) and 1355 (2050) for overheating hours and 989 (TMY) and 2797 (2050) for degree hours.

5.2.2 Window preservation scenario

Figure 6 presents the effect of the CCAMs on the average, maximum and minimum numbers of overheating

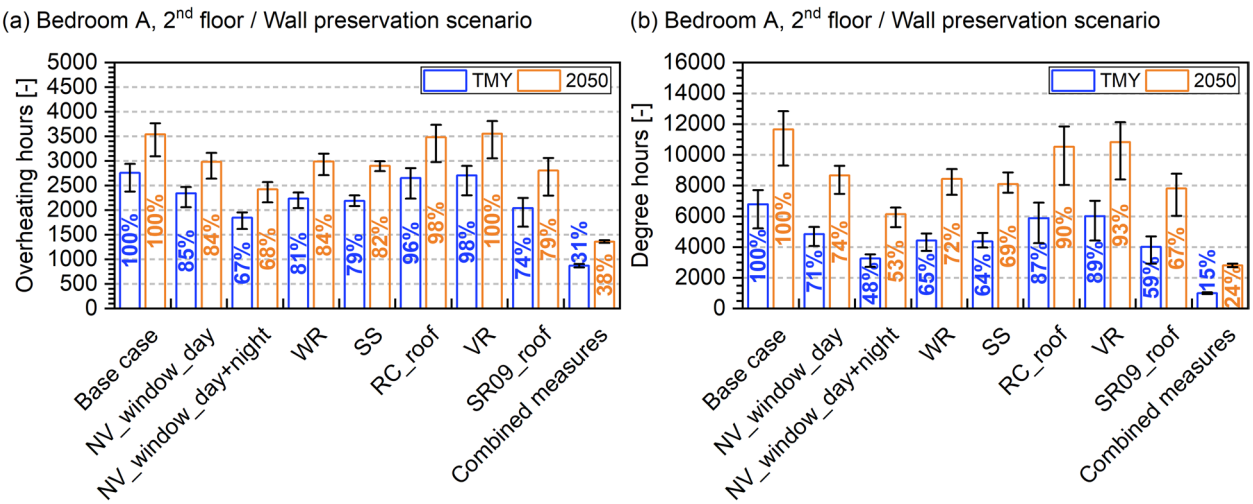

Fig. 5 Effect of climate change adaptation measures (CCAMs) on indoor overheating in the wall preservation scenario for Bedroom A on the 2nd floor in the TMY and 2050. **a** The number of overheating hours, and (**b**) the number of degree hours. NV_window_day/day + night: additional natural ventilation through windows. WR: window replacement. SS: exterior solar shading. RC_roof: increased roof insulation. VR: vegetated roof. SR09_roof: increased roof short-wave reflectance (Source: the authors)

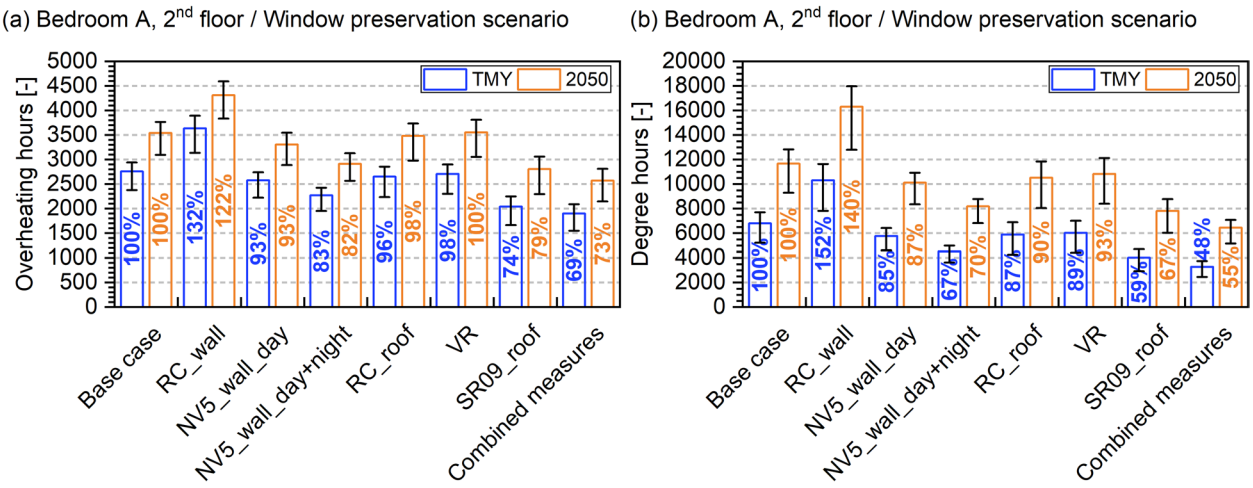

Fig. 6 Effect of CCAMs on indoor overheating in the window preservation scenario for Bedroom A on the 2nd floor in the TMY and 2050. **a** The number of overheating hours, and **b** the number of degree hours. RC_wall: increased wall insulation. NV5_wall_day/day + night: additional natural ventilation through wall openings. RC_roof: increased roof insulation. VR: vegetated roof. SR09_roof: increased roof short-wave reflectance (Source: the authors)

hours (Fig. 6a) and degree hours (Fig. 6b) in the window preservation scenario. The columns show the average values, and the error bars represent the maximum and minimum values of the eight orientations.

CCAMs for wall: In contrast to the other individual CCAMs, RC_wall increases the average number of overheating hours and degree hours. The increased indoor overheating can be explained by the increased wall insulation, which reduces the heat release through the wall to the outside when the outdoor air temperature is lower than the indoor air temperature, e.g. during the night (e.g. van Hooff et al. 2014). Similar to NV_window_day/day + night, natural ventilation through wall openings with a ventilation flow rate of 5.0 h^{-1} ACH is more effective if available for a whole day (NV5_wall_day + night) than for daytime only (NV5_wall_day). However, NV5_wall_day/day + night is less effective compared to NV_window_day/day + night.

CCAMs for roof: The same results for the CCAMs as listed for the roof in the wall preservation scenario (see Sect. 5.2.1).

Combined wall and roof CCAMs: Only a moderate reduction in the average number of overheating hours and degree hours is obtained when using the combined wall and roof CCAMs, i.e., the reduction is slightly larger than SR09_roof. For SR09_roof, the reduction is −26% (TMY) and −21% (2050) for the average number of overheating hours and −41% (TMY) and −33% (2050) for the average number of degree hours.

In the window preservation scenario, the most effective individual climate change adaptation measure is SR09_roof, and the combined wall and roof CCAMs are more effective than the individual CCAMs in terms of reducing the average number of overheating hours (−31% for TMY; −27% for 2050) and degree hours (−52% for TMY; −45% for 2050).

5.2.3 Roof preservation scenario

Figure 7 shows the effect of the CCAMs on the average, maximum and minimum numbers of overheating hours (Fig. 7a) and degree hours (Fig. 7b) in the roof preservation scenario. In Fig. 7, the columns show the average values, and the error bars represent the maximum and minimum values of the eight orientations.

CCAMs for wall: The effect of RC_wall is the same as in the window preservation scenario (see Sect. 5.2.2).

CCAMs for window: Same as the effects of CCAMs for windows in the wall preservation scenario (see Sect. 5.2.1).

Combined wall and windows CCAMs: A large reduction in the average number of overheating hours and degree hours is achieved using the combined wall and window CCAMs.

In the roof preservation scenario, the most effective individual climate change adaptation measure to reduce the average number of overheating hours is NV_window_day + night (−33% for TMY; −32% for 2050) and degree hours (−52% for TMY; −47% for 2050). Compared to the individual CCAMs, the combined wall and window CCAMs are more effective in reducing the average number of overheating hours (−53% for TMY;

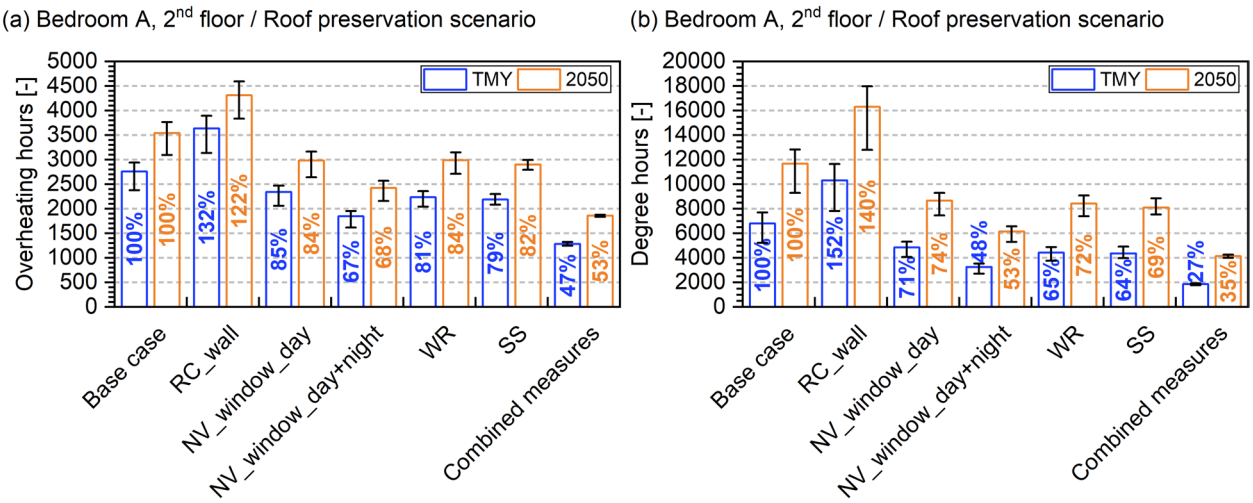

Fig. 7 Effect of CCAMs on indoor overheating in the roof preservation scenario for Bedroom A on the 2nd floor in the TMY and 2050. **a** The number of overheating hours, and (**b**) the number of degree hours. RC_wall: increased wall insulation. NV_window_day/day + night: additional natural ventilation through windows. WR: window replacement. SS: exterior solar shading (Source: the authors)

−47% for 2050) and degree hours (−73% for TMY; −65% for 2050).

5.2.4 Indoor overheating between different preservation scenarios

A comparison of the reduction in the average number of overheating hours and degree hours by using the combined measures between the three different preservation scenarios shows that the reduction for wall preservation scenario > roof preservation scenario > window preservation scenario, i.e. the remaining average number of overheating hours and degree hours is the largest for the window preservation scenario, followed by the roof preservation scenario, and finally the wall preservation scenario.

The largest remaining average number of overheating hours and degree hours occurs for the window preservation scenario due to the unchanged low-performance window (see Sect. 2), resulting in a large amount of incident solar radiation. The remaining average number of overheating hours and degree hours is larger for the roof preservation scenario than the wall preservation scenario due to the effect of the roof attic, i.e., the low albedo of the roof surface and the low thermal resistance of the roof surface and the ceiling for the dwelling on the 2nd floor (see Sect. 2).

6 Discussion

6.1 Effect of climate change adaptation measures

The larger reduction in the average number of overheating hours and degree hours achieved by using natural ventilation for a whole day, regardless of through window or wall, highlights the importance of night ventilation to reduce indoor overheating. Applying exterior solar shading limits the effect of orientation on indoor overheating.

Applying RC_roof and VR only lead to a small or even no effect on the average number of overheating hours and degree hours. Hence, given the thickness of the insulation material, i.e., 120 mm for RC_roof, and the additional actions required for using VR (e.g. MOHURD 2013), RC_roof and VR are less practical solutions for the studied dwellings to reduce indoor overheating.

In contrast to RC_roof, RC_wall increases the average number of overheating hours and degree hours. This is due to solar heat gains through the transparent surfaces of the building envelope, i.e. the windows, and the reduced transmission heat losses with increased wall insulation (e.g. van Hooff et al. 2014). Relatively small decreases in the average number of overheating hours and degree hours are found when using NV5_wall_day/day + night, and thus, mechanical ventilation may be involved to further reduce indoor overheating.

6.2 Effect of the preservation scenarios

The application of five types of commonly used CCAMs for building renovation was influenced by preservation constraints. The difference between the renovation of heritage-listed dwellings and non-heritage-listed dwellings is that some building components will have preservation constraints due to the conveyed cultural significance.

A study for non-heritage-listed dwellings showed that exterior solar shading and additional natural ventilation

were most effective in reducing indoor overheating, e.g. reducing the number of overheating hours to almost zero (van Hooff et al. 2014). However, in the window preservation scenario where the application of exterior solar shading and additional natural ventilation through the windows is constrained, a maximum reduction of 31% (TMY) and 27% (2050) for the average number of overheating hours is found. This relatively small reduction can be attributed to the effect of the preservation scenarios on the application of CCAMs.

6.3 Limitations and future work

This study used RCP8.5 in 2050 to obtain future weather data. Additional emission scenarios, e.g. RCP2.6, climate change scenarios, e.g. shared socioeconomic pathway (SSP) (O'Neill et al. 2014; Riahi et al. 2017), and other future years could be considered to address the uncertainty in future weather predictions.

In addition, for heritage preservation, other residential building types, such as detached dwellings or other building typologies for the *lilong* houses, e.g. garden-style *lilong* houses (e.g. Xu and Yan 1983), if heritage-listed, could be included in future studies. Furthermore, future work could include multiple preservation scenarios for components in the building envelope or the information regarding cultural significance conveyed to the dwellings based on the documents related to heritage designation to analyse the effect of CCAMs on cultural significance. Other aspects, e.g. CO_2 emissions, financial feasibility, and hygrothermal effects within the envelope, could be the focus of future studies. Definitions from other sources, e.g. from Historic England, that conservation refers to 'the process of maintaining and managing change to a heritage asset in a way that sustains and, where appropriate, enhances its significance' (Historic England 2024, p. 36), can be included to guide the renovation of heritage-listed dwellings in future studies. Finally, an analysis of urban interventions could be conducted, e.g. adding green infrastructure to reduce outside air temperature and solar radiation on the building envelope and subsequently achieve a possible reduction in indoor overheating.

7 Conclusions

This article investigates the climate change adaptation of Shanghai heritage-listed apartment-style *lilong* houses based on five types of CCAMs to reduce indoor overheating under RCP8.5 in 2050. The conclusions are:

- For the base case dwellings, the number of overheating hours and degree hours is larger for 2050 compared to the TMY (e.g., up to + 32% for the average number of overheating hours). Moreover, the number of overheating hours and degree hours is larger for the 2nd floor than the 1st floor (e.g. up to + 7% for the average number of overheating hours).
- Night ventilation is important for indoor overheating mitigation, whether provided through windows or wall openings.
- The effect of orientation on indoor overheating can be limited using exterior solar shading.
- Increasing roof insulation and applying the vegetated roof only result in a small or even no reduction in indoor overheating.
- The average number of overheating hours and degree hours is increased by the increased wall insulation while decreased by the increased roof insulation.
- Natural ventilation through the wall openings results in a relatively small reduction in the average number of overheating hours and degree hours compared to natural ventilation through the windows.

The most effective individual climate change adaptation measure to reduce indoor overheating for this particular case is natural ventilation through the windows for a whole day in the wall and roof preservation scenarios (−33% for TMY and −32% for 2050 for the average number of overheating hours), and increased roof albedo in the window preservation scenario (−26% for TMY and −21% for 2050 for the average number of overheating hours).

The combined CCAMs are, as expected, more effective than the individual CCAMs in all of the three preservation scenarios, with a reduction of up to 69% in the average number of overheating hours in wall preservation scenario, 31% in window preservation scenario, and 53% in roof preservation scenario. The reduction in the average number of degree hours is up to 85% in the wall preservation scenario, 52% in the window preservation scenario, and 73% in the roof preservation scenario.

This research confirms that the renovation of heritage-listed dwellings can significantly contribute to climate change adaptation and the decarbonisation of the built environment. Even if all CCAMs combined can be applied, which would be the most efficient, this research proves that a tailored approach per building and preservation constraints can lead to greater contributions by heritage-listed dwellings.

Abbreviations

ACH	Air changes per hour
AQSIQ	General Administration of Quality Supervision Inspection and Quarantine of the People's Republic of China
ASHRAE	American Society of Heating, Refrigerating and Air-Conditioning Engineers
B	Bathroom

BA	Bedroom A
BB	Bedroom B
C	Corridor
CCAM	Climate change adaptation measure
CEN	European Committee for Standardization
CIBSDR	China Institute of Building Standard Design & Research
CIBSE	The Chartered Institution of Building Services Engineers
CMA	China Meteorological Administration
CTNARCC	China's Third National Assessment Report on Climate Change
d	Cavity width
E	East
G_h	Hourly solar radiation
h_d	Degree hours
h_o	Overheating hours
ICOMOS	International Council on Monuments and Sites
K	Kitchen
LAI	Leaf area index
MOHURD	Ministry of Housing and Urban–Rural Development of the People's Republic of China
N	North
n	Number of hours during the non-heating period
NE	Northeast
NV	Additional natural ventilation
NV_wall	Additional natural ventilation through wall openings
NV_window	Additional natural ventilation through windows
NV_window_day	Additional natural ventilation through windows for daytime
NV_window_day + night	Additional natural ventilation through windows for a whole day
NV5_wall_day	Additional natural ventilation through wall openings for daytime
NV5_wall_day + night	Additional natural ventilation through wall openings for a whole day
NW	Northwest
oh_i	Hourly overheating conditions
R	Thermal resistance
R_c	Thermal resistance of construction
RC_roof	Increased roof insulation
RC_wall	Increased wall insulation
R_{cav}	Thermal resistance of the cavity
RCP	Representative concentration pathway
R_e	Exterior surface heat transfer resistance
R_i	Interior surface heat transfer resistance
S	South
SE	Southeast
SMPC	Shanghai Municipal People's Congress
SR09_roof	Increased roof short-wave reflectance
SRES	Special report on emissions scenarios
SS	Exterior solar shading
SSP	Shared socioeconomic pathway
SW	Southwest
T_a	Air temperature
TARP	Thermal Analysis Research Program
$T_{avg,2050}$	Annual average air temperature for 2050
$T_{avg,TMY}$	Annual average air temperature for the typical meteorological year
TMY	Typical meteorological year
T_o	Indoor operative temperature
T_{od-n}	Daily average outdoor temperature of n days ago
T_{rm}	Running mean outdoor temperature
T_{upper}	Upper threshold of the indoor operative temperature
U	Thermal transmittance
VR	Vegetated roof
W	West
WR	Window replacement
$\Delta G_{h,a}$	Percentual increase of the annual average hourly solar radiation from the typical meteorological year to 2050
Δn_{30}	Increase in the number of hours with air temperature > 30 °C
Δn_{35}	Increase in the number of hours with air temperature > 35 °C

Acknowledgements
The China Scholarship Council is acknowledged for the financial support.

Authors' contributions
All authors read and approved the final manuscript.

Funding
This work was financially supported by the China Scholarship Council (Grant No. 201606130059).

Data availability
The datasets used and/or analysed during the current study are available from the corresponding author on reasonable request.

Declarations

Ethics approval and consent to participate
Not applicable.

Consent for publication
Not applicable.

Competing interests
The authors declare that they have no competing interests.

Author details
[1]Unit Building Physics and Services, Department of the Built Environment, Eindhoven University of Technology, P.O. Box 513, Eindhoven 5600MB, The Netherlands. [2]Unit Architectural Urban Design and Engineering, Department of the Built Environment, Eindhoven University of Technology, Eindhoven, The Netherlands. [3]Institute of Mechanical, Process and Energy Engineering, School of Engineering and Physical Sciences, Heriot-Watt University, Edinburgh, Scotland, UK. [4]Building Physics and Sustainable Design, Department of Civil Engineering, KU Leuven, Leuven, Belgium. [5]Department of Architectural Engineering & Technology, Faculty of Architecture and the Built Environment, Delft University of Technology, Delft, The Netherlands.

Received: 26 September 2023 Revised: 20 February 2025 Accepted: 4 March 2025
Published online: 25 April 2025

References

Albers, R.A.W., P.R. Bosch, B. Blocken, A.A.J.F. van den Dobbelsteen, L.W.A. van Hove, T.J.M. Spit, F. van de Ven, T. van Hooff, and V. Rovers. 2015. Overview of challenges and achievements in the climate adaptation of cities and in the Climate Proof Cities program. *Building and Environment* 83: 1–10. https://doi.org/10.1016/j.buildenv.2014.09.006.

AQSIQ (General Administration of Quality Supervision Inspection and Quarantine of the People's Republic of China) and SAC (Standardization Administration of the People's Republic of China). 2008. *Ergonomics of the thermal environment - Determination of metabolic rate (GB/T 18048–2008/ ISO 8996: 2004)*. [In Chinese.] Beijing: Standards Press of China.

ASHRAE (American Society of Heating Refrigerating and Air-Conditioning Engineers). 2021. *2021 ASHRAE Handbook - Fundamentals*. SI. Peachtree Corners, GA, USA: American Society of Heating, Refrigerating and Air-Conditioning Engineers Inc.

Australia ICOMOS. 2013. *The Burra Charter: The Australia ICOMOS Charter for Places of Cultural Significance*. https://australia.icomos.org/wp-content/uploads/The-Burra-Charter-2013-Adopted-31.10.2013.pdf. Accessed 25 Mar 2023.

Baba, F.M., H. Ge, L. (Leon) Wang, and R. Zmeureanu. 2023. Assessing and mitigating overheating risk in existing Canadian school buildings under

extreme current and future climates. *Energy and Buildings* 279: 112710. https://doi.org/10.1016/j.enbuild.2022.112710.

Barbosa, R., R. Vicente, and R. Santos. 2015. Climate change and thermal comfort in Southern Europe housing: A case study from Lisbon. *Building and Environment* 92: 440–451. https://doi.org/10.1016/j.buildenv.2015.05.019.

Beck, W., D. Dolmans, G. Dutoo, A. Hall, and O. Seppänen. 2010. *REHVA Guidebook No. 12 - Solar Shading - How to Integrate Solar Shading in Sustainable Buildings*. Brussels, Belgium: REHVA (the Federation of European Heating, Ventilation and Air Conditioning Associations).

Bretz, S., H. Akbari, A. Rosenfeld, and H. Taha. 1992. *Implementation of solar-reflective surfaces: materials and utility programs*. Report number: LBL-32467. Energy Analysis Program, Energy & Environment Division, Lawrence Berkeley Laboratory. Berkeley, CA: University of California. https://doi.org/10.2172/10172670.

Carlucci, S., L. Bai, R. de Dear, and L. Yang. 2018. Review of adaptive thermal comfort models in built environmental regulatory documents. *Building and Environment* 137: 73–89. https://doi.org/10.1016/j.buildenv.2018.03.053.

CECS (China Association for Engineering Construction Standardization). 2010. *Technical specification for kitchen and bathroom of medium-small apartments (CECS 284: 2010).* [In Chinese.] Beijing: China Planning Press.

CEN (European Committee for Standardization). 2007. *EN ISO 6946: 2007 - Building components and building elements - Thermal resistance and thermal transmittance - Calculation method*. Brussels: European Committee for Standardization.

Climate Change Center of CMA (China Meteorological Administration). 2019. *China Blue Book on Climate Change (2019).* [In Chinese.] Beijing: Climate Change Center of China Meteorological Administration.

Chen, S., M.D. Levine, H. Li, P. Yowargana, and L. Xie. 2012. Measured air tightness performance of residential buildings in North China and its influence on district space heating energy use. *Energy and Buildings* 51: 157–164. https://doi.org/10.1016/j.enbuild.2012.05.004.

Chen, H., W.L. Lee, and X. Wang. 2015. Energy assessment of office buildings in China using China building energy codes and LEED 2.2. *Energy and Buildings* 86: 514–524. https://doi.org/10.1016/j.enbuild.2014.10.034.

CIBSDR (China Institute of Building Standard Design & Research). 2014. *Planting roofing construction (14J206).* [In Chinese.] Beijing: China Planning Press.

CIBSE (The Chartered Institution of Building Services Engineers). 2015. *Environmental Design - CIBSE Guide A*, 8th ed. London: CIBSE.

Crawley, D.B., L.K. Lawrie, F.C. Winkelmann, W.F. Buhl, Y.J. Huang, C.O. Pedersen, R.K. Strand, R.J. Liesen, D.E. Fisher, M.J. Witte, and J. Glazer. 2001. EnergyPlus: Creating a new-generation building energy simulation program. *Energy and Buildings* 33 (4): 319–331. https://doi.org/10.1016/S0378-7788(00)00114-6.

CTNARCC (China's Third National Assessment Report on Climate Change) Editorial Committee. 2015. *China's Third National Assessment Report on Climate Change.* [In Chinese.] Beijing: Science Press.

De Berardinis, P., M. Rotilio, C. Marchionni, and A. Friedman. 2014. Improving the energy-efficiency of historic masonry buildings. A case study: A minor centre in the Abruzzo region, Italy. *Energy and Buildings* 80 (September): 415–423. https://doi.org/10.1016/j.enbuild.2014.05.047.

Feng, C., Q. Meng, N. Li, and Y. Zhang. 2010. Study on radiative properties of Sedum lineare. [In Chinese.] *Building Science* 26 (4): 65–68. https://doi.org/10.13614/j.cnki.11-1962/tu.2010.04.004.

Hasan, A., J. Kurnitski, and K. Jokiranta. 2009. A combined low temperature water heating system consisting of radiators and floor heating. *Energy and Buildings* 41 (5): 470–479. https://doi.org/10.1016/j.enbuild.2008.11.016.

Historic England. 2024. *Adapting Historic Buildings for Energy and Carbon Efficiency*. https://historicengland.org.uk/images-books/publications/adapting-historic-buildings-energy-carbon-efficiency-advice-note-18/heag321-adapting-historic-buildings-energy-carbon-efficiency/. Accessed 22 Sept 2024.

Hu, S., D. Yan, J. An, S. Guo, and M. Qian. 2019. Investigation and analysis of Chinese residential building occupancy with large-scale questionnaire surveys. *Energy and Buildings* 193: 289–304. https://doi.org/10.1016/j.enbuild.2019.04.007.

Jafarpur, P., and U. Berardi. 2021. Effects of climate changes on building energy demand and thermal comfort in Canadian office buildings adopting different temperature setpoints. *Journal of Building Engineering* 42: 102725. https://doi.org/10.1016/j.jobe.2021.102725.

Lam, J.C., C.L. Tsang, D.H.W. Li, and S.O. Cheung. 2005. Residential building envelope heat gain and cooling energy requirements. *Energy* 30 (7): 933–951. https://doi.org/10.1016/j.energy.2004.07.001.

LBL (Lawrence Berkeley Laboratory). 1994. *DOE2.1E-053 source code*.

Lei, M., T. van Hooff, B. Blocken, and A. Pereira Roders. 2022. The predicted effect of climate change on indoor overheating of heritage apartments in two different Chinese climate zones. *Indoor and Built Environment* 31 (7): 1986–2006. https://doi.org/10.1177/1420326X221085861.

Lianjia. 2016. *Pre-owned housing of Yongjia New Village.* [In Chinese.] https://sh.lianjia.com/ershoufang/107010076903.html. Accessed 27 Oct 2019.

Liu, B.Y.H., and R.C. Jordan. 1963. The long-term average performance of flat-plate solar-energy collectors: with design data for the U.S., its outlying possessions and Canada. *Solar Energy* 7 (2): 53–74. https://doi.org/10.1016/0038-092X(63)90006-9.

Lou, C., and S. Xue. 2002. *Laoshanghai Jingdian Jianzhu* [Old Shanghai Classic Buildings]. [In Chinese.] Shanghai: Tongji University Press.

Martínez-Molina, A., I. Tort-Ausina, S. Cho, and J.-L. Vivancos. 2016. Energy efficiency and thermal comfort in historic buildings: A review. *Renewable and Sustainable Energy Reviews* 61: 70–85. https://doi.org/10.1016/j.rser.2016.03.018.

Meteotest. 2020a. *Meteonorm Handbook part I: Software*. Global Meteorological Database Version 8 Software and Data for Engineers, Planers and Education. https://meteonorm.com/assets/downloads/mn80_software.pdf. Accessed 13 Feb 2021.

Meteotest. 2020b. *Meteonorm Handbook part II: Theory*. Global Meteorological Database Version 8 Software and Data for Engineers, Planers and Education. https://meteonorm.com/assets/downloads/mn80_theory.pdf. Accessed 13 Feb 2021.

Meteotest. 2021. *Meteonorm Software (version 8.0.3)*. https://meteonorm.com/. Accessed 13 Feb 2021.

Mirsadeghi, M., D. Cóstola, B. Blocken, and J.L.M. Hensen. 2013. Review of external convective heat transfer coefficient models in building energy simulation programs: Implementation and uncertainty. *Applied Thermal Engineering* 56 (1–2): 134–151. https://doi.org/10.1016/j.applthermaleng.2013.03.003.

MOHURD (Ministry of Housing and Urban-Rural Development of the People's Republic of China) and AQSIQ (General Administration of Quality Supervision Inspection and Quarantine of the People's Republic of China). 2012a. *Evaluation standard for indoor thermal environment in civil buildings (GB/T 50785–2012).* [In Chinese.] Beijing: China Architecture & Building Press.

MOHURD (Ministry of Housing and Urban-Rural Development of the People's Republic of China) and AQSIQ (General Administration of Quality Supervision Inspection and Quarantine of the People's Republic of China). 2012b. *Standard for daylighting design of buildings (GB 50033–2013).* [In Chinese.] Beijing: China Architecture & Building Press.

MOHURD (Ministry of Housing and Urban-Rural Development of the People's Republic of China) and AQSIQ (General Administration of Quality Supervision Inspection and Quarantine of the People's Republic of China). 2016. *Code for Thermal Design of Civil Building (GB 50176–2016).* [In Chinese.] Beijing: China Architecture & Building Press.

MOHURD (Ministry of Housing and Urban-Rural Development of the People's Republic of China). 2010. *Design standard for energy efficiency of residential buildings in hot summer and cold winter zone (JGJ 134–2010).* [In Chinese.] Beijing: China Architecture & Building Press.

MOHURD (Ministry of Housing and Urban-Rural Development of the People's Republic of China). 2012. *Technical specification for energy efficiency retrofitting of existing residential buildings (JGJ/T 129–2012).* [In Chinese.] Beijing: China Architecture & Building Press.

MOHURD (Ministry of Housing and Urban-Rural Development of the People's Republic of China). 2013. *Technical specification for green roof (JGJ 155–2013).* [In Chinese.] Beijing: China Architecture & Building Press.

MOHURD (Ministry of Housing and Urban-Rural Development of the People's Republic of China). 2018. *Design standard for energy efficiency of residential buildings in severe cold and cold zones (JGJ 26–2018).* [In Chinese.] Beijing: China Architecture & Building Press.

Moss, R.H., J.A. Edmonds, K.A. Hibbard, M.R. Manning, S.K. Rose, D.P. van Vuuren, T.R. Carter, S. Emori, M. Kainuma, T. Kram, G.A. Meehl, J.F.B. Mitchell, N. Nakicenovic, K. Riahi, S.J. Smith, R.J. Stouffer, A.M. Thomson, J.P. Weyant, and T.J. Wilbanks. 2010. The next generation of scenarios for climate

change research and assessment. *Nature* 463 (7282): 747–756. https://doi.org/10.1038/nature08823.
Muñoz González, C.M., A.L. León Rodríguez, R. Suárez Medina, and J. Ruiz Jaramillo. 2020. Effects of future climate change on the preservation of artworks, thermal comfort and energy consumption in historic buildings. *Applied Energy* 276: 115483. https://doi.org/10.1016/j.apenergy.2020.115483.
O'Neill, B.C., E. Kriegler, K. Riahi, K.L. Ebi, S. Hallegatte, T.R. Carter, R. Mathur, and D.P. van Vuuren. 2014. A new scenario framework for climate change research: The concept of shared socioeconomic pathways. *Climatic Change* 122 (3): 387–400. https://doi.org/10.1007/s10584-013-0905-2.
Office of Shanghai Chronicles. 2005. *Shanghai Mingjianzhu Zhi*. [In Chinese.] Shanghai, China: Shanghai Academy of Social Sciences Press.
Peng, M., and Z. Yang. 2019. Cooling and humidification effect of green roof on the outdoor microclimate. [In Chinese.] *Journal of Civil and Environmental Engineering* 41 (4)*:* 165–173. https://doi.org/10.11835/j.issn.2096-6717.2019.085.
Riahi, K., D.P. van Vuuren, E. Kriegler, J. Edmonds, B.C. O'Neill, S. Fujimori, N. Bauer et al. 2017. The Shared Socioeconomic Pathways and their energy, land use, and greenhouse gas emissions implications: An overview. *Global Environmental Change* 42: 153–168. https://doi.org/10.1016/j.gloenvcha.2016.05.009.
Sailor, D., and B. Bass. 2014. Development and Features of the Green Roof Energy Calculator (GREC). *Journal of Living Architecture* 1 (3): 36–58. https://doi.org/10.46534/jliv.2014.01.03.036
Shi, S., C. Chen, and B. Zhao. 2015. Air infiltration rate distributions of residences in Beijing. *Building and Environment* 92: 528–537. https://doi.org/10.1016/j.buildenv.2015.05.027.
Song, D., and Y. Chen. 2010. The renovation of Shanghai Alleys from dual angles of historic preservation and ecological energy saving. [In Chinese.] *Housing Science* 30 (1): 55–59. https://doi.org/10.13626/j.cnki.hs.2010.01.003.
Song, D., and H. Mo. 2010. Study on reconstruction strategy of ecological human settlement of Shanghai's lane buildings. [In Chinese.] *Housing Science* 30 (4): 51–54. https://doi.org/10.13626/j.cnki.hs.2010.04.006.
Standing Committee of SMPC (Shanghai Municipal People's Congress). 2019. *Regulations on the preservation of Shanghai historical areas and heritage architecture*. [In Chinese.]
Tang, M., Z. Yang, and K. Zheng. 2007. Thermal R-values of green roof. [In Chinese.] *Journal of Chongqing University (Natural Science Edition)* 30 (5): 1–3. https://doi.org/10.11835/j.issn.1000-582X.2007.05.001.
Thevenard, D., and K. Haddad. 2006. Ground reflectivity in the context of building energy simulation. *Energy and Buildings* 38 (8): 972–980. https://doi.org/10.1016/j.enbuild.2005.11.007.
U.S. Department of Energy. 2019a. *EnergyPlus*. https://energyplus.net/. Accessed 16 Feb 2019.
U.S. Department of Energy. 2019b. *EnergyPlus Version 9.1.0 documentation: Engineering Reference*.
U.S. Department of Energy. 2019c. *EnergyPlus Version 9.1.0 documentation: Input Output Reference*.
van Hooff, T., B. Blocken, J.L.M. Hensen, and H.J.P. Timmermans. 2014. On the predicted effectiveness of climate adaptation measures for residential buildings. *Building and Environment* 82: 300–316. https://doi.org/10.1016/j.buildenv.2014.08.027.
van Vuuren, D.P., J. Edmonds, M. Kainuma, K. Riahi, A. Thomson, K. Hibbard, G.C. Hurtt, T. Kram, V. Krey, J.-F. Lamarque, T. Masui, M. Meinshausen, N. Nakicenovic, S.J. Smith, and S.K. Rose. 2011. The representative concentration pathways: An overview. *Climatic Change* 109 (1–2): 5–31. https://doi.org/10.1007/s10584-011-0148-z.
Vasaturo, R., T. van Hooff, I. Kalkman, B. Blocken, and P. van Wesemael. 2018. Impact of passive climate adaptation measures and building orientation on the energy demand of a detached lightweight semi-portable building. *Building Simulation* 11 (6): 1163–1177.
Walton, G.N. 1983. *Thermal analysis research program reference manual. NBSIR 83–2655*. U.S. Department of Commerce, National Bureau of Standards, National Engineering Laboratory, Building Physics Division, Washington, DC, USA. March 1983.
Xu, J., and W. Yan. 1983. Historical development, preservation and renovation of Shanghai Lilong dwellings. [In Chinese.] *Housing Science* 6: 8–11.
Xue, S., and C. Lou. 2005. *Laoshanghai Jingdian Gongyu* [Old Shanghai Classic Apartments]. [In Chinese.] Shanghai: Tongji University Press.
Xuhui District Housing Security and Administration Bureau. 2016. *Reply on the restoration plan of Yongjia Xincun outstanding historic building, Lane 580, Yongjia Road*. http://xxgk.xh.sh.cn/WebSite/HTML/xhxxgk/xxgk_fgj_bmwj_bmwj/Info/Detail_17139.htm. Accessed 18 Sept 2024.
Yu, Y., Y. Shao, B. Zhao, J. Yu, H. Guo, and Y. Chen. 2023. Study on Summer Overheating of Residential Buildings in the Severe Cold Region of China in View of Climate Change. *Buildings* 13 (1): 244. https://doi.org/10.3390/buildings13010244.

Publisher's Note